Pergamon

PII: S0277-5387(97)00200-3

*Polyhedron* Vol. 16, No. 24, pp. 4371–4378, 1997
© 1997 Elsevier Science Ltd
All rights reserved. Printed in Great Britain
0277-5387/97 $17.00+0.00

# The crystal structures and electrochemical studies of two naphthalenic Schiff base copper(II) complexes

Juan M. Fernández-G.,[a]* Ma. del Rocío Patiño-Maya,[a] Rubén A. Toscano,[a] Luis Velasco,[a] Martha Otero-López[b] and Martha Aguilar-Martínez[b]

[a]Instituto de Química, U.N.A.M., Circuito Exterior. Cd. Universitaria, Coyoacán 04510, México D.F., México

[b]Departamento de Fisicoquímica, División de Estudios de Posgrado, Facultad de Química, U.N.A.M., Cd. Universitaria, Coyoacán 04510, México D.F., México

(Received 17 January 1997; accepted 9 May 1997)

**Abstract**—The Schiff base ligands, 2-hydroxy-N-cyclohexyl-1-naphthaldimine (**I**), and 3-hydroxy-N-cyclohexyl-2-naphthaldimine (**II**), and their corresponding $Cu^{II}$ complexes (**1**–**2**) respectively were synthesized and characterized. The crystal and molecular structures of bis-{(cyclohexyl)[(2-oxo-1H-naphth-1-ylidene)-methyl]aminato}copper(II) (**1**) and bis-{(cyclohexyl)[(3-oxo-2H-naphth-2-ylidene)-methyl]aminato} copper(II) (**2**), were determined. The X-ray diffraction study shows that the geometry around the metal atom for (**1**), is stepped square planar with a step of 1.063 Å while for (**2**), the geometry around the metal atom is distorted square planar with an angle between the coordination planes O(1)—Cu—N(1) and O(1a)—Cu—N(1a) of 39.9°. Electrochemical studies show a dependence of the $Cu^{II}/Cu^{I}$ potentials on the ligand structure. © 1997 Elsevier Science Ltd

*Keywords*: copper(II) complexes; naphthalenic Schiff base complexes; crystal structure; electrochemical studies; voltammetry.

Metal Schiff base complexes derived from salicylaldehyde have been extensively studied [1–4]. However, there are few structural studies on complexes of Schiff bases derived from 2-hydroxy-1-naphthalenecarboxaldehyde [5–13] and even fewer copper(II) complexes derived from 3-hydroxy-2-naphthalenecarboxaldehyde [14,15]. Considering that it is important to develop the available structural data of closely related systems as happens with complexes derived of salicylaldamines, 2-hydroxy-1-naphthaldimines and 3-hydroxy-2-naphthaldimines. This paper, reports the synthesis and characterization of two naphthaldimines where a cyclohexyl group is bonded to the imine nitrogen of each ligand, i.e.: 2-hydroxy-N-cyclohexyl-1-naphthaldimine (**I**), and 3-hydroxy-N-cyclohexyl-2-naphthaldimine (**II**), and their corresponding coordination copper(II) compounds bis-{(cyclohexyl)[(2-oxo-1H-naphth-1-ylidene)-methyl]aminato}copper(II) (**1**) and bis-{(cyclohexyl)[(3-oxo-2H-naphth-2-ylidene)-methyl]-aminato}copper(II) (**2**), respectively. Single crystal X-ray analysis of the complexes (**1**) and (**2**) was undertaken in order to elucidate the conformation and structure of both complexes, examine the possible conformational differences between them, and compare both of them with the structure of the brown form of the salicylaldehyde copper(II) homolog (**3**) already described [16]. Finally, cyclic voltammetry and other measurements were also carried out for complexes (**1**)–(**3**) in order to explore the dependence of the $Cu^{II}/Cu^{I}$ potentials on the structure and electronic variations of the ligands.

## EXPERIMENTAL

Melting points were determined on a Fisher–Johns melting point apparatus and are uncorrected; infrared spectra (KBr disks) were recorded on a Perkin–Elmer

---

* Author to whom correspondence should be addressed.

Mod. 203-B spectrometer, UV–vis spectra on a Perkin–Elmer Mod. 552 spectrophotometer, mass spectra for the ligands, were obtained using a Hewlett–Packard instrument Mod. 5985, at 70 eV ionizing potential; for the complexes, positive fast atom bombardment mass spectra were obtained on a JEOL Mod. JMS-SX-102A mass spectrometer operated at an accelerating voltage of 10 kV. Samples were disorbed from nitrobenzyl alcohol matrix using xenon atoms at 6 KeV; NMR spectra in a Varian Gemini 200 using $CDCl_3$ as solvent; magnetic moment measurements were made with a Johnson Matthey magnetic susceptibility balance at 24°C. Elemental analyses were performed by Galbraith Laboratories, Inc. Knoxville, Tenn. 37921-1750, U.S.A.

The following chemicals: 2-hydroxy-1-naphthalenecarboxaldehyde, cyclohexylamine, salicylaldehyde, copper(II) acetate monohydrate, phosphorus pentachloride, naphthol AS, tin(II) chloride anhydrous and N,N-dimethylformamide (DMF) spectroscopic grade, were from Aldrich Chemical Co. Inc., and were used without further purification, tetra-n-ethylammonium tetrafluoroborate ($Et_4NBF_4$) was from Fluka, 3-hydroxy-2-naphthalenecarboxaldehyde was prepared as described in literature [17] using Naphthol AS as starting material. Ligands and copper complexes were prepared by methods described elsewhere [18–19]. Compound (**3**) was obtained by a template procedure obtaining a brown crystalline solid with m.p. 167–169°C (lit. 165–166°C) [16]. Additionally, (**3**) was characterized by its mass spectrum, showing a $M^+$ peak at 468 $m/z$ with the characteristic $(M^+ + 2)$ isotopic contribution of copper.

Electrochemistry. Cyclic voltammetric and double potential step chronocoulometry measurements [20,21] were carried out with a Bioanalytical Systems Inc. 100 B/W Electrochemical Workstation instrument equipped with a three-electrode system. The working electrode used was a platinum disk (2 mm diameter). The reference electrode used was a saturated calomel electrode (SCE), separated from the bulk of the solution by a bridge filled with solvent and supporting electrolyte. Solutions in the bridge were changed periodically to avoid aqueous contamination from entering the cell via the SCE. The auxiliary electrode was a Pt-wire. $Et_4NBF_4$ 0.1 M was used as supporting electrolyte and DMF as solvent. The electroactivity range for this system was 3.6 V (from 1.6 to −2.0 V *vs* SCE). For cyclic voltammetry and chronocoulometry the concentration of copper(II) complexes was 1 mM in the electrolytic medium. All measurements were carried out at room temperature under an atmosphere of nitrogen, and the solutions were recently prepared before use. Prior to taking measurements, the solutions were purged with nitrogen satu-

Table 1. Summary of crystal and intensity collection data for compounds (**1**) and (**2**)

| Compound | (**1**) | (**2**) |
|---|---|---|
| Formula | $C_{34}H_{36}N_2O_2Cu$ | $C_{34}H_{36}N_2O_2Cu$ |
| Molecular weight | 568.2 | 568.2 |
| Crystal system | Monoclinic | Monoclinic |
| Space group | $P2_1/n$ | $C2/c$ |
| Crystal colour | Dark red-brown | Dark red-brown |
| $T$ (K) | 293 | 298 |
| $\lambda$ (Mo-K$\alpha$) | 0.71073 Å | 0.71073 Å |
| Scan mode | $\omega$ | $2\theta:\theta$ |
| Crystal dimensions (MM) | 0.26 × 0.24 × 0.44 | 0.26 × 0.30 × 0.42 |
| $a$ (Å) | 6.133(2) | 18.937(8) |
| $b$ (Å) | 10.827(2) | 12.836(3) |
| $c$ (Å) | 20.929(5) | 11.446(2) |
| $\beta$ (°) | 98.46(2) | 97.19(3) |
| $V$ (Å$^3$) | 1374.5(5) | 2760.4(1.4) |
| $hkl$ ranges | $0 < h < 7$ | $0 < h < 22$ |
| | $0 < k < 12$ | $0 < k < 15$ |
| | $-24 < l < 24$ | $-12 < l < 12$ |
| $\rho_{calc.}$ (Mgm$^{-3}$) | 1.373 | 1.367 |
| $Z$ | 2 | 4 |
| $F(000)$ | 598 | 1196 |
| $\mu$ cm$^{-1}$ | 8.29 | 8.24 |
| $2\theta$ range (°) | 3–50 | 3–50 |
| $R$ | 0.0520 | 0.037 |
| $R_w$ | 0.0564 | 0.038 |
| Unique reflections collected | 2419 | 2459 |
| Observed reflections | 1433 | 2124 |
| | $[F_o > 4\sigma(F_o)]$ | $[F_o > 3\sigma(F_o)]$ |

rated with solvent vapor for *ca* 15 min in order to remove dissolved oxygen. Cyclic voltammograms were measured with variable sweep rates between 0.01 and $-10.24$ V sec$^{-1}$ and iR drop was compensated. During chronocoulometry experiments a pulse width of 10 msec was applied. Controlled-potential electrolysis measurements [22] were carried out on a PAR model 175 potentiostat/galvanostat, using as a working electrode a platinum plate of an area of 4 cm$^2$.

Suitable X-ray-quality crystals of (**1**) and (**2**) were grown by slow layer diffusion of MeOH into a $CH_2Cl_2$ solution. The crystals were mounted on a glass fiber and diffraction experiments were performed on a Nicolet P3F four-circle diffractometer with graphite-monochromated Mo-K$\alpha$ radiation. In both cases, orientation matrices and lattice parameters were obtained from the least-squares refinements of the setting angles of 25 reflections ($4.0 < 2\theta < 25.0°$). Crystal data, and additional data collection parameters are given in Table 1. The data sets were collected up to $\sin\theta/\lambda = 0.5946$, and three standard reflections were recorded every 100 reflections. Lorentz and polarization corrections were applied to both data sets and absorption corrections ignored. The observed extinctions and subsequent refinements confirmed the respective space groups.

The atomic scattering factors were taken from International Tables for X-Ray Crystallography [23]. The structures were solved by direct methods employing the SHELXTL PLUS PC Version package [24]. The refinements were carried out by using block-matrix least-squares techniques on *F*, minimizing the function $\omega[|F_o| - |F_c|]^2$ where the weight $\omega$, is defined as $[\sigma^2(F_o) + gF_o^2]^{-1}$ [$g = 0.0008$ for (**1**) and 0.0006 for (**2**)]. In the final cycles of refinement all non-hydrogen atoms were refined anisotropically. In all cases, hydrogen atom positions were forced to ride the parent C-atom assuming a C—H bond length of 0.96 Å and its temperature factors were fixed at a constant value $U_{iso} = 0.06$ Å$^2$ and included in the refinement. The largest peaks in the final difference Fourier map calculations showed residual electron densities of no chemical significance.

## RESULTS AND DISCUSSION

Some physical properties of the synthesized compounds are showed in Table 2. All compounds are soluble in dichloromethane or chloroform, but the complexes are less soluble than the ligands in other solvents such as: alcohols, tetrahydrofuran, benzene and ethyl acetate. The elemental analyses were satisfactory and show the complexes have a ligand-to-metal ratio of 2:1. Mass spectra of ligands and complexes show the expected molecular ions, the molecular ions in the mass spectra of complexes show the characteristic copper isotopic distribution, which agrees with the 2:1 ligand to metal stoichiometric ratio. The NMR spectra for the ligands show signals characteristic of the naphthalene rings and the cyclohexyl substituents; there are two signals at low field, the one at lower field (around 13–14 ppm) disappears with $D_2O$ and can be attributed to the phe-

Table 2. Colour, melting points, molecular ion, magnetic moments, NMR and UV–vis bands of the prepared compounds

| Compound | Colour | m.p (°C) | $M^+$ [Base peak] ($m/z$) | $\mu_{eff}$ (B.M.) | NMR[c] (in ppm) | UV–vis[d] (in cm$^{-1}$) [$\varepsilon$] |
|---|---|---|---|---|---|---|
| **I**[a] | Yellow | 68–70 | 253 [170] | — | 1.2–2.0 m; 3.35 m; 6.87–7.81 m; 8.6 s; 14.5 s | 41,841 [28,550], 38,168 [13,271], 36,900 [9036], 32,573 [10,447], 24,938 [8659], 23,810 [9036]. |
| **1**[b] | Brown–red | 196–198 | 568 [154] | 1.80 | — | 37,736 [24,421], 37,175 [23,493] sh*, 33,003 [20,870], 26,178 [12,976] sh*, 25,189 [15,352], 23,923 [10,107] sh*. |
| **II**[a] | Pale yellow | 126–28 | 253 [253] | — | 1.2–1.9 m; 3.22–3.36 m; 7.2–7.8 m; 8.53 s; 13.3 s | 39,683 [42,916], 38,911 [43,572], 35,971 [9473] sh*, 34,364 [8714] sh*, 33,113 [7449], 29,586 [8433], 27,100 [1462], 23,041 [255] sh* |
| **2**[a] | Brown–red | 250–52 | 568 [154] | 1.81 | — | 39,682 [74,646], 38,461 [79,102], 36,765 [55,796] sh*, 33,445 [34,537], 31,949 [24,510] sh*, 23,364 [4648]. |

[a] UV–vis in $CHCl_3$.
[b] UV–vis in DMF.
[c] m, multiplet; s, singlet.
[d] sh*, shoulder.

Table 3. Selected bond lengths (Å) and angles (°) for (**1**) and (**2**) with e.s.d.'s in the least significant figure given in parentheses

| Compound (**1**) | | Compound (**2**) | |
|---|---|---|---|
| Cu—O(1) | 1.883(3) | Cu—O(1) | 1.886(2) |
| Cu—N(1) | 1.999(4) | Cu—N(1) | 1.992(2) |
| O(1)—C(2) | 1.306(7) | O(1)—C(3) | 1.326(3) |
| N(1)—C(11) | 1.284(6) | N(1)—C(11) | 1.286(3) |
| N(1)—C(12) | 1.494(6) | N(1)—C(12) | 1.492(3) |
| C(1)—C(2) | 1.407(8) | C(1)—C(2) | 1.390(3) |
| C(2)—C(3) | 1.437(7) | C(2)—C(3) | 1.439(3) |
| C(1)—C(11) | 1.440(7) | C(2)—C(11) | 1.446(4) |
| N(1)—Cu—N(1a) | 180.0(1) | N(1)—Cu—N(1a) | 152.3(1) |
| O(1)—Cu—N(1) | 89.5(2) | N(1)—Cu—O(1) | 94.6(1) |
| N(1)—Cu—O(1a) | 90.5(2) | N(1)—Cu—O(1a) | 92.6(1) |
| O(1)—Cu—N(1a) | 90.5(2) | O(1)—Cu—N(1a) | 94.6(1) |
| O(1)—Cu—O(1a) | 180.0(1) | O(1)—Cu(1)—O(1a) | 149.7(1) |
| O(1)—C(2)—C(1) | 124.4(4) | O(1)—C(3)—C(2) | 121.7(2) |
| N(1)—C(11)—C(1) | 127.2(5) | N(1)—C(11)—C(2) | 127.3(2) |
| Cu—N(1)—C(11) | 123.8(3) | Cu—N(1)—C(11) | 122.6(2) |
| Cu—N(1)—C(12) | 118.1(3) | Cu—N(1)—C(12) | 117.3(1) |
| Cu—O(1)—C(2), | 128.2(3) | Cu—O(1)—C(3) | 128.9(2) |
| C(11)—N(1)—C(12) | 118.1(4) | C(11)—N(1)—C(12) | 120.1(2) |

nolic proton. The other one (around 8.6 ppm) is assigned to the proton bonded to the carbon atom of the imine group. The values of magnetic moments for both complexes (Table 2) are slightly smaller than the values described for planar n-alkyl-salicylidenaminato copper(II) complexes as in the range 1.83–1.86 BM [25]. The infrared spectra of ligands show the characteristic $\nu$(O—H) absorption bands around 3400 cm$^{-1}$ which disappears after complexation, the absorption corresponding to the $\nu$(—C═N—) vibration is around 1620 cm$^{-1}$ in the ligands, and in the complexes it is shifted approximately 15 cm$^{-1}$ to a lower wave number as described in similar complexes [26]. The electronic spectra of the complexes show only intraligand or charge transfer bands (see Table 2).

A selection of bond lengths and angles is given in Table 3. The molecular structures of the compounds (**1**) and (**2**) including atom-numbering schemes, are illustrated in Figs 1 and 2, respectively.

The X-ray diffraction analyses of the complexes (**1**) and (**2**) show, in both cases, that the copper ion is bonded to the oxygen and nitrogen donor atoms of the two ligand molecules in a trans arrangement in which the copper ion is four coordinate. The geometry in (**1**) is stepped square planar with a step of 1.063 Å, while in (**2**) it is distorted square planar where the angle between the two coordination planes defined by O(1)—Cu—N(1) and O(1a)—Cu—N(1a) is 39.9°. Bond angles also show that the coordination geometry about the copper atom in (**1**) is square planar and in (**2**) distorted square planar. With O—Cu—N, N—Cu—N and O—Cu—O angles of 90.5(2)°, 180.0(1)°, 180.0(1)° and 92.6(1)°, 152.3(1)°, 149.7(1)°, respectively. Other angles show expected values.

The Cu—O and Cu—N bonds in (**1**) and (**2**), have similar lengths and are in the same range to those reported for similar bis-(1,2-naphthaldaminato) copper complexes i.e. Cu—O distances are in the range 1.87(1)–1.922(3) Å, while Cu—N distances have values between 1.962(4) and 2.002(3) Å [6–10], the analogous salicylidenaminato copper complex (**3**) shows Cu—O and Cu—N bond lengths of 1.896(2) and 2.034(2), respectively [16]. Finally, the C(1)—C(2), C(2)—C(3) and the imine C(11)—N(1) bond lengths are also similar for both (**1**) and (**2**).

It is worthy of mention, that the geometry around the Cu$^{II}$ ion in (**1**) is quite similar to that reported for (**3**) [16], in which the structure is stepped square planar with a step of 1.28 Å slightly larger than the value of 1.063 Å for (**1**), while (**2**) deviates from this situation since its geometry is distorted square planar. In fact, the only difference between (**1**) and (**2**) is the difference in the bond order or charge density of positions 1,2 and 2,3 of the naphthalene rings which might be responsible for that deviation from the square planar symmetry in (**2**) or as another alternative, packing effects in the crystalline state could be responsible for that distortion, but should only be observed in the solid state.

The redox behaviour of the three Schiff base copper(II) complexes was preliminarily examined by cyclic voltammetry. All (**1**)–(**3**) complexes were found to have very similar cyclic voltammograms. Table 4 summarises the potentials which depend on the structure and ligand electron density. The cyclic voltammogram (Fig. 3a, b) of compound (**1**) illustrates this general behaviour. The Cu$^{II}$L/Cu$^{I}$L reduction potential occurred at −832 mV *vs* SCE, peak A, and has a quasi-reversible behaviour as indicated by the non-equivalent current intensity of cathodic and

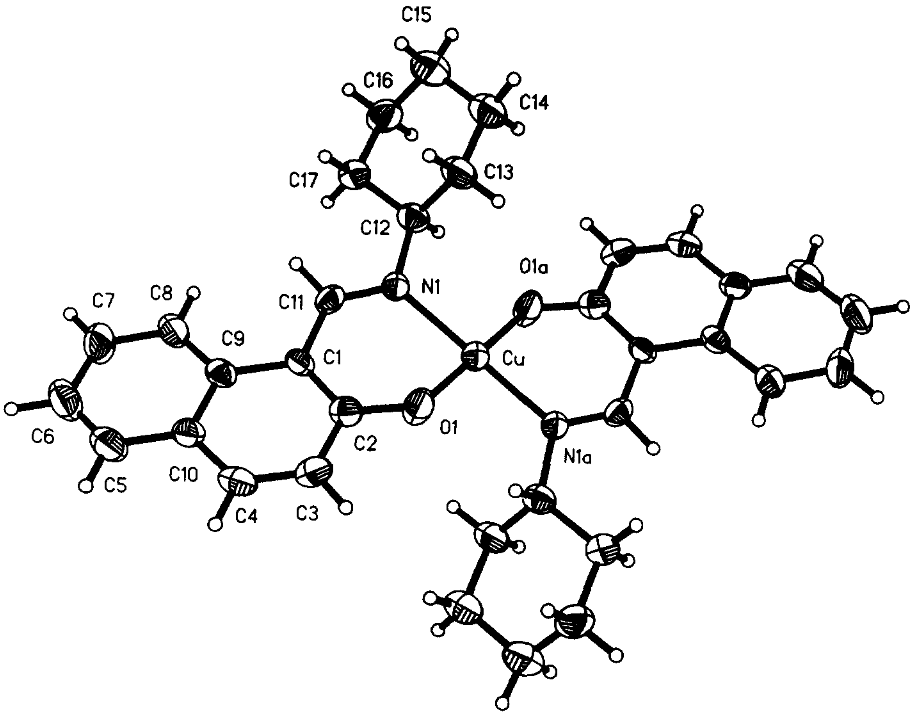

Fig. 1. The molecular structure of (**1**) with the atom numbering scheme. Thermal ellipsoids are drawn at 50% probability.

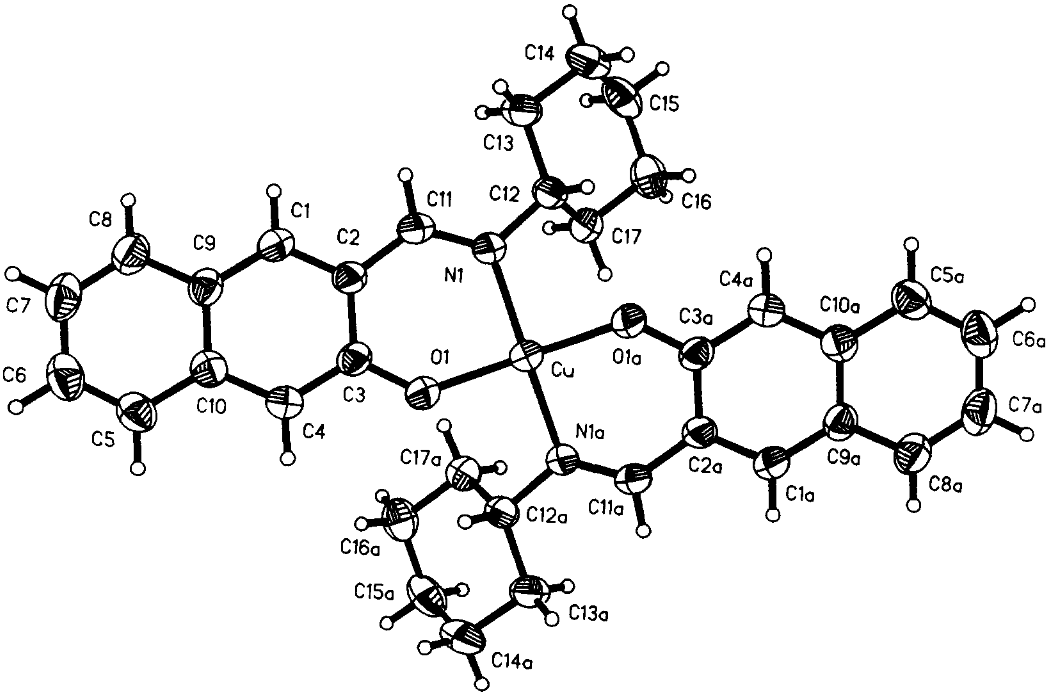

Fig. 2. The molecular structure of (**2**) with the atom numbering scheme. Thermal ellipsoids are drawn at 50% probability.

anodic peaks ($i_{pa}/i_{pc} = 0.717$) and the greater loss in current intensity of the anodic wave relative to the cathodic wave at faster scan rates (Figure 4). The quasi-reversible character of this couple was also shown by the large separation between anodic and cathodic peaks of 131 mV at 100 mV s$^{-1}$ (Table 4, Fig. 3b). Furthermore, the observed linear relationship between cathodic current ($i_{pc}$) and the square root of the sweep rate ($v^{1/2}$), shown in Fig. 5 for (**1**), indicates a diffusion-controlled electrochemical process. Similar behaviour was observed for the other complexes.

Table 4. Electrochemical parameters[a] and chemical homogeneous rate constants[b] for the cathodic reduction of compounds (**1**), (**2**) and (**3**) in DMF solution

| Compound | $E_{pc}$ (mV) | $E_{pa}$ (mV) | $\Delta E_p$/mV | $i_{pa}/i_{pc}$ | $k_s \times 10^{-4}$ (cm sec$^{-1}$) | $k \times 10^{-5}$ (sec$^{-1}$) |
|---|---|---|---|---|---|---|
| (**1**) | −832 | −701 | 131 | 0.717 | 7.541 | 5.776 |
| (**2**) | −774 | −651 | 123 | 0.607 | 4.583 | 3.025 |
| (**3**) | −869 | −686 | 183 | 0.485 | 3.524 | 5.390 |

[a] Measured at 100 mV s$^{-1}$.

[b] Measured by double potential step chronocoulometry.

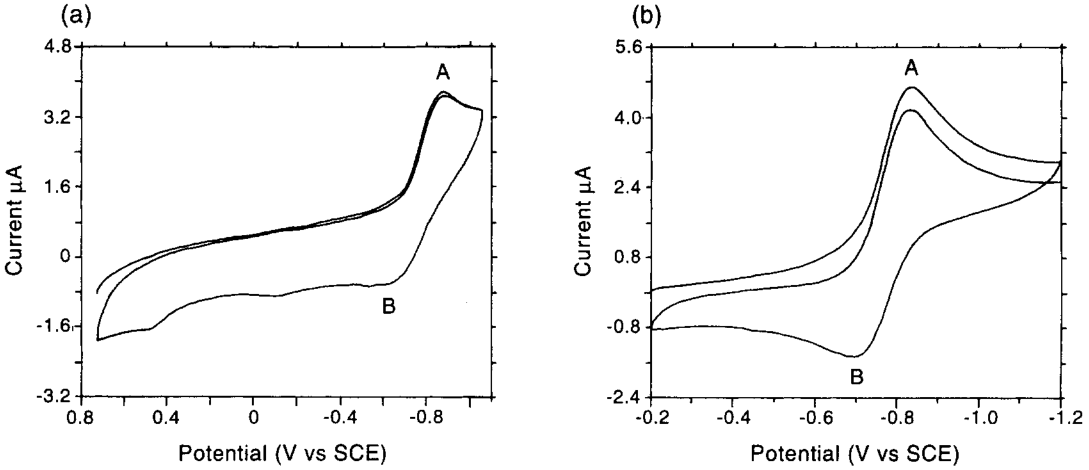

Fig. 3. Cyclic voltammogram recorded at a platinum electrode in DMF solution containing complex (**1**) ($1.0 \times 10^{-3}$ mol dm$^{-3}$) and $Et_4NBF_4$ (0.1 mol dm$^{-3}$); scan rate 100 mV s$^{-1}$. Starting potential (a) 0.65 V; (b) −0.2 V.

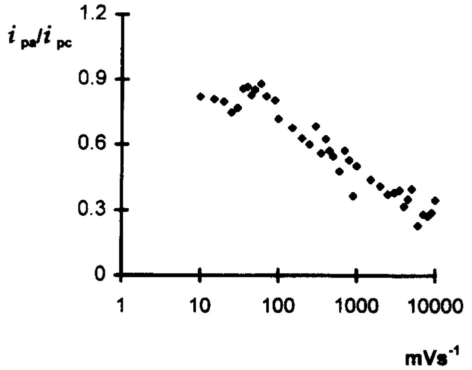

Fig. 4. Plot of the ratio of anodic to cathodic peak currents, cathodic current ($i_{pa}/i_{pc}$) as a function of scan rate.

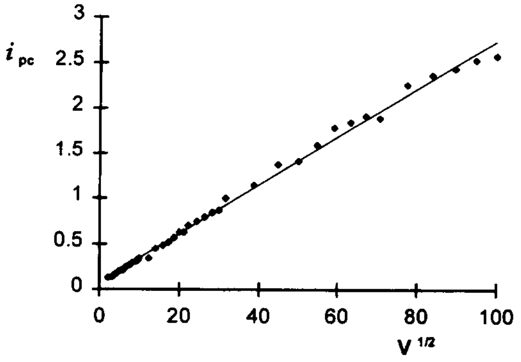

Fig. 5. Cathodic current ($i_{pc}$) *vs* square root of sweep rate ($v^{1/2}$) for complex (**1**).

The heterogeneous electrochemical rate constant ($k_s$) and the homogeneous chemical rate constant (k) were obtained by cyclic voltammetry [27] and chronocoulometry [28], respectively, for the system Cu$^{I}$-$^{I}$L/Cu$^{I}$L, $k_s$ values are into the range of quasi-reversible systems, $10^{-1} < k_s < 10^{-5}$ cm sec$^{-1}$, in which the slow electron transfer kinetics could be due to intramolecular structural changes due to a follow up chemical reaction characteristic of an EC mechanism. The presence of a chemical reaction after the reduction of Cu$^{II}$L was made evident by the homogeneous chemical rate constant k, with a value of $5.77 \times 10^{-5}$ sec$^{-1}$ for compound (**1**), which lies between 0 and $10^3$ sec$^{-1}$, characteristic of a slow chemical reaction [29]. Studies of related compounds [30–32] have pointed out that, in order to decrease the energy of the reduction process, it is necessary to generate a highly distorted ligand field around the copper(II) ion or to surround it with an extended $\pi$ electron system. The last statement agrees with our

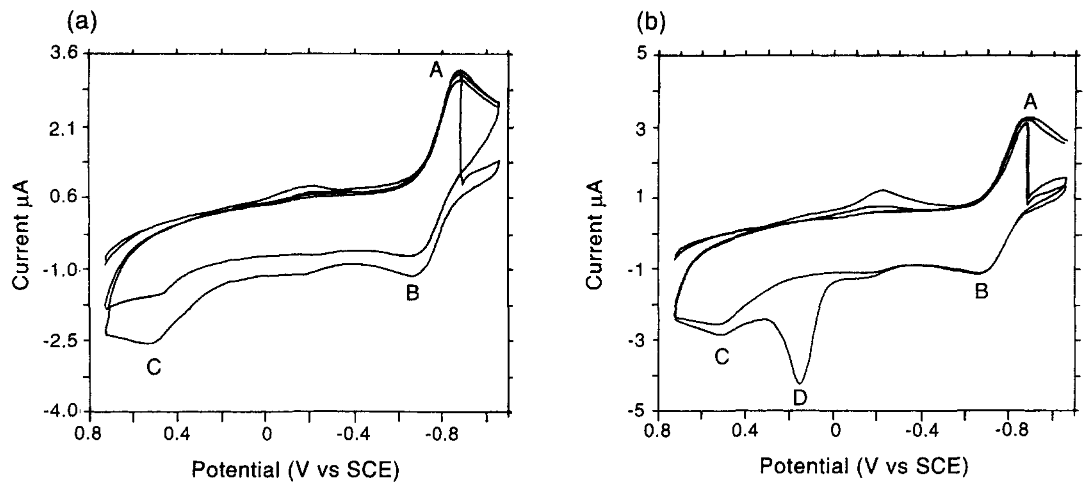

Fig. 6. Cyclic voltammogram recorded at a platinum electrode in DMF solution containing complex (**1**) ($1.0 \times 10^{-3}$ mol dm$^{-3}$) showing the oxidation of Cu$^0$ and Cu$^{+1}$ and Cu$^{+2}$. Controlled potential at −770 mV *vs* SCE, for (a) 1 min; (b) 2 min.

work, as we have found that the $E_{pc}$ decreased in the following order (**3**) > (**1**) > (**2**) (Table 4). An extra aromatic ring in compound (**1**) with respect to compound (**3**) decreased the reduction potential by 37 mV. Moreover, when going from (**1**) to (**2**), both being isomeric compounds and having the same number of rings, the reduction potential decreased by 58 mV which means that the facility for reducing (**2**) could be explained by a smaller charge density on the naphthalene C(2)—C(3) positions of the ligand with respect to that found at C(1)—C(2) in (**1**) in which the ligand is able to exert a stronger electronic effect toward the metal center. Even if we do not have the charge density values for compounds (**1**) and (**2**), it is possible to relate them to the values calculated for similar nickel complexes [33].

It has been reported that the occurrence of a relatively slow electron transfer, quasi-reversible in electrochemical terms [34], is indicative of important stereochemical reorganizations. The electron transfer from Cu$^{\mathrm{I}}$L to Cu$^0$L was not observed within the cathodic interval measured (from 0 to −2.0 V *vs* SCE) at the scan rates studied. It is well known that in some cases the relevant copper(I) species are unestable and subsequently decompose to copper metal [30], this is probably due to the fact that the first reduction step must be accompanied by demetallation of the complex, as illustrated by the reoxidation of copper metal to free Cu$^{+1}$ and Cu$^{+2}$ ions and shown by the presence of peaks C and D (Fig. 6a and b), respectively. Peak C appeared only during the second scan after the reduction step, Cu$^{\mathrm{II}}$L to Cu$^{\mathrm{I}}$L $E_{pc} = -832$ mV (peak A). This may be explained considering that some Cu$^{\mathrm{I}}$L is able to be reoxidated to Cu$^{\mathrm{II}}$L $E_{pa} = -701$ mV (peak B) but some of it may be decomposed to free Cu$^{+1}$ ion which was oxidated to Cu$^{+2}$ ion at peak C, $E_{pa} = 520$ mV. This last step was demonstrated by the presence of a chemical follow up reaction with a homogeneous chemical rate constant $k = 5.77 \times 10^{-5}$ sec$^{-1}$. Peak C notably increased when the scan was stopped at the potential peak A for 1 min. It is noticeable that after holding the potential at −832 mV for 2 min, enough Cu$^{\mathrm{I}}$L was produced to quickly decompose to Cu$^0$ with the destruction of the complex. In addition, Cu$^0$ was further reoxidated to Cu$^{+1}$ ion giving rise to peak D, $E_{pa} = 157$ mV (Fig. 6b). That Cu$^{\mathrm{I}}$L is easily decomposed to Cu$^0$, was proved when, at the beginning of the controlled-potential electrolysis ($E_w = -832$ mV) of compound (**1**), the current increased notably, but after a few minutes it dropped dramatically and the Pt cathode was covered by metallic copper. As a result of this experiment the number of electrons involved in this step could not be determined.

As a concluding remark we can see that while (**1**) is square planar, (**2**) is distorted square planar and the reduction potential of (**2**) is smaller than that of (**1**). This agrees with reported voltammetric studies on copper(II) complexes where it is indicated that non-planar complexes are easier to reduce than their planar analogs [30]. Also, the information obtained in this study in the solid state by X-ray diffraction, as in solution by electrochemistry point to the same conclusion that is: the differences in stereochemistries and reduction potentials between (**1**) and (**2**) might be explained only in terms of an electronic effect.

To better understand the structural and electrochemical differences between copper(II) complexes derived of salicylaldamines, 2-hydroxy-1-naphthaldimines and 3-hydroxy-2-naphthaldimines, we are undertaking a more systematic investigation of these compounds.

*Acknowledgements*—We thank Mr Jair Domínguez-Ceronio and Mr Abelardo Cuellar for technical assistance.

*Supplementary material for compounds* (**1**) *and* (**2**). Packing arrangement; atom coordinates; complete bond lengths and angles; anisotropic temperature factors, and hydrogen coordinates. Equations for least squares planes and observed and calculated structure factors. These data are available from the Editor on request.

## REFERENCES

1. Holm, R. H. and O'Connor, M. J., *Prog. Inorg. Chem.*, 1971, **14,** 241.
2. Maslen, H. S. and Waters, T. N., *Coord. Chem. Rev.*, 1975, **17,** 137.
3. Panova, G. V., Vikulova, N. K. and Potapov, V. M., *Russian Chem. Rev.*, 1980, **49,** 655.
4. Garnovskii, A. D., Nivorozhin, A. L. and Minkin, V. I., *Coord. Chem. Rev.*, 1993, **126,** 1.
5. Shnulin, A. N., Mamedov, Kh. S. and Struchkov, Yu. T., *Z. Struck. Khim.*, 1978, **19,** 686.
6. Clark, G. R., Waters, T. N. and Williams, G. J., *J. Inorg. Nucl. Chem.*, 1977, **39,** 1971.
7. Clark, G. R., Waters, J. M. and Waters, T. N., *J. Inorg. Nucl. Chem.*, 1975, **37,** 2455.
8. Martin, D. W. and Waters, T. N., *J. Chem. Soc., Dalton Trans.*, 1973, 2440.
9. Matsumoto, N., Nonaka, Y., Kida, S., Kawano, S. and Ueda, I., *Inorg. Chim. Acta*, 1979, **37,** 27.
10. Maniukiewicz, W. and Bukovska-Strzyzewska, M., *J. Cryst. Spectrosc. Res.*, 1990, **20,** 363.
11. Elerman, Y., Paulus, E. F. and Fuess, H., *Acta Cryst.*, 1991, **C47,** 70.
12. Elerman, Y., Fuess, H. and Paulus, E. F., *Acta Cryst.*, 1992, **C48,** 40.
13. Hökelek, T., Gùndüz, N., Hayvali, Z. and Kilic, Z., *Acta Cryst.*, 1995, **C51,** 880.
14. Fernández-G., J. M., Lembrino-Canales, J. J. and Villena-I., R., *Monats. Chem.*, 1994, **125,** 275.
15. Fernández-G., J. M. and Lembrino-Canales, J. J., *Monats. Chem.*, 1995, **126,** 129.
16. Tamura, H., Ogawa, K., Takeuchi, A. and Yamada, S., *Chem. Letters*, 1977, 889.
17. Khorana, M. L. and Pandit, S. Y., *J. Indian Chem. Soc.*, 1963, **40,** 789.
18. Vogel, A. I., *Practical Organic Chemistry*, pp. 653–654. Longmans, London (1966).
19. Yamada, S., Kuge, K. and Yamagouchi, K., *Bull. Chem. Soc. Jap.*, 1967, **40,** 1864.
20. Heinze, J., *Angew, Chem. Int. Ed. Engl.*, 1984, **23,** 831.
21. Heineman, W. R. and Kissinger, P. T., *Laboratory Techniques in Electroanalytical Chemistry*, Chap. 3, Marcel Dekker, New York (1984).
22. Mann, C. K., *Instrumental Analysis*, Harper & Row, New York (1980).
23. Cromer, D. T. and Waber, J. T., *International Tables for X-Ray Crystallography*, Vol. IV, Table 2.2A, the Kynoch Press, Birmingham, England (1974).
24. Sheldrick, G. M., 1990. SHELXTL/PC User's Manual. Siemens Analytical X-rays Instruments, Inc., Madison, Wisconsin, U.S.A.
25. Sacconi, L. and Ciampolini, M., *J. Chem. Soc.*, 1964, 276.
26. Kovacic, J. E., *Spectrochim. Acta*, 1967, **23A,** 183.
27. Nicholson, R. S., *Anal. Chem.*, 1965, **37,** 1351.
28. Christie, J. H., *J. Electroanal. Chem.*, 1967, **13,** 79.
29. Geiger, W. E., *Prog. Inorg. Chem.*, 1985, **33,** 275.
30. Patterson, G. S. and Holm, R. H., *Bioinorg. Chem.*, 1975, **4,** 257.
31. Costamagna, J., Vargas, J., Latorre, R., Alvarado, A. and Mena, G., *Coord. Chem. Rev.*, 1993, **119,** 67.
32. Bursten, B. E. and Green, M. R., *Prog. Inorg. Chem.*, 1988, **36,** 393.
33. Fernández-G., J. M., Rosales-Hoz, M. J., Rubio-Arroyo, M. F., Salcedo, R., Toscano, R. A. and Vela, A., *Inorg. Chem.*, 1987, **26,** 349.
34. Bard, A. J. and Faulkner, L. R., *Electrochemical Methods. Fundamentals and Applications*, John Wiley, New York (1980).